Density functional theory applied to VN/TiN multilayers

P. Lazar* and J. Redinger
Institut für Allgemeine Physik, Technische Universität Wien, Getreidemarkt 9, A-1060 Vienna, Austria

R. Podloucky
Institut für Physikalische Chemie, Universität Wien, Sensengasse 8, A-1090 Vienna, Austria

(Received 8 August 2007; revised manuscript received 18 October 2007; published 26 November 2007)

By means of a density functional theory approach, materials properties of VN[001](100)‖TiN[001](100) multilayers are studied focusing on the elastic and mechanical properties of the interface. For the isolated bulk phases of TiN and VN, elastic constants and moduli are derived in order to analyze the matching conditions at the interface. Modeling of the mechanical properties was done in terms of brittle cleavage by calculating cleavage energies and critical stresses for the bulk phases as well as for the multilayer system. The interface energy of -0.054 J/m^2 was derived for the lateral lattice parameter of MgO(100) according to the multilayer growth on this substrate. For this case, also atomic interlayer distances and critical stresses are determined and a Poisson ratio of the VN[001] and TiN[001] was evaluated. The values of $\nu=0.279$ and $\nu=0.235$, respectively, agree very well with the available experimental data. The strain energy and the interfacial cleavage properties of the multilayer are calculated as a function of the lateral lattice parameter illustrating growth conditions on different substrates. The cleavage energy at the interface considerably changes with respect to the lateral lattice parameter, but the critical stress of ≈ 27 GPa remains rather unchanged. The relaxation of atoms following an epitaxial strain of VN layers transforms VN into the structure with tetragonal-like stacking. This fact is an indication that stoichiometric VN is *metastable* against tetragonal distortion.

DOI: 10.1103/PhysRevB.76.174112 PACS number(s): 73.21.Ac, 68.65.Ac, 71.15.Nc, 81.15.Aa

I. INTRODUCTION

Experiments demonstrated that multilayered coatings composed of transition metal nitrides exhibit a hardness larger than 40 GPa, which is larger than for coatings of the constituent monophase nitrides.[1–3] Such coatings are promising for applications in which high hardness and wear resistances are needed. VN/TiN phases may reach hardness of 56 GPa (Ref. 1) and techniques for such coatings (e.g., magnetron sputtering) may reach industrially relevant deposition rates.

The hardness enhancement of multilayered phases is a complex phenomenon and, therefore, it is not well understood. Several models have been proposed. Shinn *et al.*[3] indicated that different elastic moduli of the constituent layer materials are needed in order to increase the hardness of a superlattice film. The approach of Chu and Barnett[4] is based on restricted dislocation glides across and inside the layers. It is argued that the important issue is the difference in shear moduli of the individual components in combination with the formation of a well defined interface. This model provides a good fit to the scarce experimental data. A variety of other properties are suggested for the hardness enhancement, such as elastic anomalies[1] or coherency strains near the interface.[2,5,6]

Theoretical studies so far aimed at metal/nonoxide ceramic interfaces, and most of the effort was devoted to interfaces with transition metal carbides. Only three density functional theory (DFT) studies considered nitride/metal interfaces. Hartford[7] derived the interfacial free energy for the Fe/VN (100) interface, considering also the effect of nitrogen vacancies. Siegel *et al.*[8,9] studied the adhesion energies for Al/(VN,CrN,TiN) interfaces, including variations in the interfacial stacking sequence. Usually coherent interfaces are studied, but misfit dislocations are within reach of DFT, as shown recently for a NiAl/Mo eutectic composite.[10]

In the present work, we apply a DFT approach in order to provide reliable atomistic data for elastic and mechanical properties of a single-crystal VN/TiN multilayer system. The multilayer orientation was chosen to be VN[001] $\times$(100)‖TiN[001](100) for several reasons: (a) [001] is the directions of the nearest neighbor bonds in the rocksalt structure, (b) cleaving (100) layers is easiest as compared to other directions, and (c) strengthening was observed in multilayer superlattices precisely with this stacking.[1]

For the isolated bulk phases of TiN and VN, elastic constants and moduli are derived in order to analyze the matching conditions at the interface. Modeling of the mechanical properties was done in terms of brittle cleavage by calculating cleavage energies and critical stresses for the bulk phases as well as for the multilayer system. The interface energy was derived for the lateral lattice parameter of MgO(100) according to the multilayer growth on this substrate. For this case, also atomic interlayer distances and critical stresses are determined. The strain energy of the multilayer is calculated as a function of the lateral lattice parameter illustrating growth conditions on different substrates.

In a first step, the isolated bulk phases are studied. Elastic constants of VN and TiN are calculated from which macroscopically averaged elastic moduli and shear moduli for polycrystalline samples are estimated. By that, reliable differences in elastic and shear moduli of both phases can be derived. Furthermore, brittle cleavage properties in terms of the cleavage energy and the critical stress are calculated for bulk VN and TiN. The cleavage energy and the critical stress are a fundamental property of the bonding in the material, and they describe the onset of brittle crack propagation as well.[11]

The VN/TiN multilayer is simulated by a periodic slab with ideal 1:1 metal and/or nitrogen stoichiometry. Defects, such as vacancies on the nitrogen sublattice, are not considered. A coherent interface is modeled, for which the lateral lattice parameter for both VN and TiN is the same. Well defined interfaces are suggested to be a requirement for the hardness enhancement, and in the case of VN/TiN multilayer were actually observed.[1] We also derive the interface energy by calculating the difference between the total energy per unit area of the multilayer system and the corresponding total energies of the bulk phases. It represents the change in chemical bonding due to the formation of the interface. Diffusional and plastic degrees of freedom, which may lower the interface energy considerably, are not taken into account.

According to elasticity theory, the formation of a coherent interface between two mismatched materials is accompanied by uniaxial strains in both parts, which results in a common value of the lateral lattice parameter. In our case, the strain energy is calculated by changing the lateral lattice parameter of the slab. By that, coherent growth on different substrates with different lateral lattice parameters may be simulated. In particular, a MgO(100) substrate, which is often used for growing epitaxial single-crystalline nitride films, (for example, Refs. 1, 12, and 13) and an Al(100) substrate is considered. Finally, we calculate the cleavage properties of the VN/TiN multilayer at the interface, similar to the study of the pure bulk phases.

II. DETAILS OF CALCULATIONS

For the DFT calculations, the Vienna *ab initio* simulation package[14,15] (VASP) was applied. The generalized gradient approximation (GGA) of Perdew and Wang[16] was chosen for parametrization of the exchange-correlation functional. Atomic forces were relaxed within the conjugate-gradient algorithm wherever structural relaxations were required.

Both TiN and VN crystallize in the cubic rocksalt structure, which was considered for all studies. For studies of the multilayer system, a suitable tetragonal cell was constructed. In all cases, the ideal 1:1 stoichiometry of metal and nitrogen is assumed, i.e., no defects were taken into account. The convergency of the total energy with respect to computational parameters such as the number of **k** points for the Brillouin zone integration was tested. An energy cutoff of 400 eV was considered to be sufficiently accurate. For the high-accuracy calculations of elastic constants and lattice parameters of the bulk phases of TiN and VN, the cutoff was increased up to 600 eV, for which also $15\times15\times15$ **k** point grid was used.

The elastic constants c_{11}, c_{12}, and c_{44} are evaluated by means of the total energy calculated as a function of suitable strains. The energy density was fitted by a polynomial ansatz, and its second derivative at the equilibrium volume was determined.

A VN/TiN multilayer of VN[001](100)‖TiN[001](100) orientation is studied. The multilayer is modeled in two ways: (a) by a periodic slab with n number of layers of VN(100) and the same number of layers of TiN(100) terminated by free surfaces (at least three vacuum layers) and (b) by periodically stacking the (100) layers, as depicted in Fig. 1.

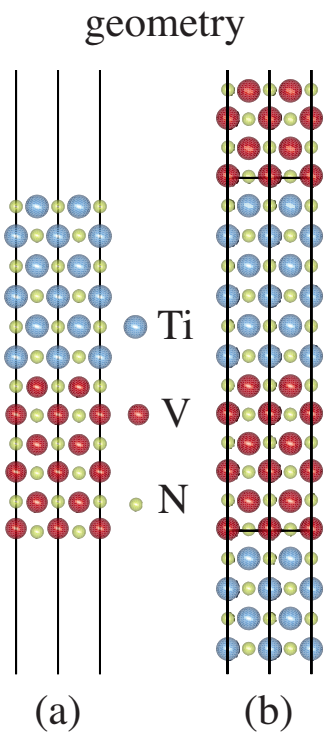

FIG. 1. (Color online) Model of the two geometries used in the calculations: (a) repeated slab with six layers of VN(100) and six layers of TiN(100) terminated by free surfaces (at minimum three vacuum layers); and (b) periodically repeated blocks of 6+6 VN/TiN(100) layers.

Convergency studies showed that six numbers of layers are sufficient for a proper modeling of the interface. Geometry (a) has the advantage that layer geometries may vary without changing the actual slab size (i.e., unit cell).

Brittle cleavage was modeled by a slab of geometry (a), as described above. Convergency of the cleavage energy as a function of the slab thickness and vacuum spacing was tested. Unit cells with six atomic layers separating the interfaces were sufficiently thick. Because the intention is to describe ideal brittle cleavage, no atomic positions were relaxed during cleaving.

Strain energies for the multilayer system were calculated making use of geometry (b).

III. VN AND TiN BULK PHASES

A. Elastic properties

Tables I and II show the lattice constants a_0, bulk moduli B_0, and elastic constants of VN and TiN, respectively.

Comparing our values of a_0 and B_0 to full-potential linearized augmented plane waves (FLAPW) results,[22] one generally realizes very good agreement, if GGA was applied. FLAPW is usually considered to provide the benchmarks. DFT calculation using the local density approximation (LDA) for the exchange-correlation functional illustrate the

TABLE I. Calculated lattice parameter a (in Å), bulk modulus B_0, and elastic constants (in GPa) for VN.

Method	a	B_0	c_{11}	c_{12}	c_{44}
Present work	4.128	320	636	162	126
GGA, FLAPW[a]	4.12	333			
LDA, FLAPW[b]	4.092	372	752	183	121
Expt.	4.13[c]	268[d]	533[d]	135[d]	133[d]

[a]Reference 17.
[b]Reference 18.
[c]$VN_{0.98}$ at 93 K (Ref. 19).
[d]VN thin film (Ref. 12).

well-known overbinding effect of LDA,[23] namely, smaller equilibrium volumes and higher values of elastic constants. For TiN, results of two other approaches—the full-potential linearized muffin tin orbital (FLMTO) method and a pseudopotential (PP) approach—also show reasonable agreement with the other data, although the equilibrium volume of the FLMTO approach is less satisfying. In comparison to experiment, there is a significant discrepancy for elastic constant c_{11}: the experimental value is about 20% smaller than our result. Presumably, the problem is the preparation of high-quality single crystals, because nitrogen vacancies are certainly of importance.

A distinct feature of cubic refractory compounds such as VN and TiN is the very large value of c_{11} (636 and 604 GPa, respectively). This elastic constant reflects the strong covalent bonds between the metal d-like states and the nitrogen p-like states along the [100] directions. This is expressed by the direction-dependent uniaxial modulus [Eq. (A1)] which is equal to c_{11} for these directions.

From the elastic constants c_{11}, c_{12}, and c_{44}, the corresponding compliances s_{11}, s_{12}, and s_{44} are obtained by method described in the Appendix. Young's modulus E in the direction of the unit vector $[hkl]$ is then evaluated by the relation[25]

$$\frac{1}{E} = s_{11} - 2\left(s_{11} - s_{12} - \frac{1}{2}s_{44}\right)(h^2k^2 + k^2l^2 + l^2h^2). \quad (1)$$

The values of the direction-dependent Young's moduli in these directions are listed in Table III. For both materials, the modulus has its maximum in the [100] direction. It should be noted, that—in contrast to TiN and VN—for most metals with cubic crystal structure the expression $\left(s_{11} - s_{12} - \frac{1}{2}s_{44}\right)$ is positive and, consequently, Young's modulus has a maximum in the [111] direction and a minimum in the [100] direction. On the other hand, an anisotropy, similar to VN and TiN, found for metallic polonium is attributed to the simple cubic structure, which is essentially a rocksalt structure if both atoms of the compounds are identical.[26] This emphasizes the common feature of both types, namely, the dominance of the first nearest neighbor interactions.

Experimentally, the elastic constants of single-crystal VN and TiN films were determined from surface acoustic wave dispersions. The values in Tables I and II were measured on films grown on MgO (100) substrates. The agreement is rather good, if one takes into account that the residual stresses—due to the lattice mismatch—are inherently present in the experimental data, and the samples might contain a certain (yet unknown) amount of defects.

For TiN, many experimental data for Young's modulus—most of them derived from hardness measurements—are available. The value of 640 GPa found for stoichiometric TiN thin film coated onto stainless steel[27] is higher than our value of Table III. However, the reported values of Young's modulus show some significant scattering. For example, the films coated by a vapor deposition technique, Young's modulus of about 400 GPa was measured.[28,29] It should be noted that for these films, x-ray diffraction and transmission electron microscopy reveal (220) and (111) preferential orientations.[30] According to Table III, the moduli in these

TABLE II. Calculated lattice parameter a (in Å), bulk modulus B_0, and elastic constants (in GPa) for TiN

Method	a	B_0	c_{11}	c_{12}	c_{44}
Present work	4.270	292	604	136	162
GGA, FLAPW[a]	4.26	286			
GGA, FLMTO[b]	4.23	270	610	100	168
LDA, FLAPW[c]	4.229	328	706	138	175
LDA, PP[d]	4.22	261	516	129	132
Expt.	4.26[e]	320	625[f]	165[f]	163[f]

[a]Reference 17.
[b]Reference 20.
[c]Reference 18.
[d]Reference 21.
[e]$TiN_{0.98}$ at 93 K (Ref. 19).
[f]TiN thin film (Ref. 12).

TABLE III. Calculated elastic compliances (in 10^{-12} m^2 N^{-1}) and direction-dependent Young's modulus E (in GPa) for three low-index directions as derived from the elastic constants in Tables I and II.

	s_{11}	s_{12}	s_{44}	$E[100]$	$E[110]$	$E[111]$
VN	1.75	−0.4	7.94	570	373	334
TiN	1.81	−0.3	6.17	554	439	410

directions are 439 and 410 GPa, respectively, now in good agreement to these experiments. Of course, a number of physical conditions are of influence for the deposition techniques, such as substrate temperature, bias voltage, nitrogen pressure, etc. The conditions during deposition may alternate preferred orientation of grains or film texture and, consequently, change the elastic properties of the film.

Because polycrystalline properties may be also of importance for coated materials, we estimated the elastic properties of polycrystalline VN and TiN samples. Several averaging procedures are in use by which the elastic moduli of a quasi-isotropic polycrystalline materials are derived from its single crystal elastic constants. The averaging is done over all orientations of the crystal with a well-defined lower and upper limit for the elastic moduli.

Inspecting the averaged elastic constants displayed in Table IV, one realizes deviation of ≈20% between the Voigt and Reuss averages. The Poisson ratio of TiN agrees well with a recent experimental result of $\nu=0.23\pm0.03$ obtained from a technique combining impact excitation and depth-sensing indentation.[31] The data for elastic properties of VN are very sparse. That makes our results particularly useful because Poisson's ratio is important for the characterization of coatings: it is used to estimate the mechanical properties of coatings in techniques such as depth-sensing indentation[32] and surface acoustic wave spectroscopy.[33] Measuring Poisson's ratio of a coating is extremely difficult and it is often assumed that Poisson's ratio of a coating is the same as that of the bulk material. In general, that may not be the case.

B. Brittle cleavage properties

Ideal brittle cleavage between planes of orientation (hkl) is described in terms of Griffith's energy balance,[11] according to which cleavage generated by load mode I (i.e., external load perpendicular to the cleavage planes) propagates when the mechanical energy release rate G exceeds the cleavage energy G_c, defined as the energy needed to separate the solid material into two blocks. The energy $G(x)$ depends on the crack size or separation x of two blocks of the material.

TABLE IV. Calculated averaged elastic constants (in GPa) of VN and TiN. Young's modulus E, shear modulus μ, and Poisson ratio ν according to the averaging procedures of Voigt and Reuss.

	Method	E	μ	ν
VN	Voigt	434	170	0.27
	Reuss	400	155	0.29
TiN	Voigt	470	191	0.23
	Reuss	458	185	0.24

We determined the brittle cleavage properties of each material by calculating total energies for a set of given fixed separations x_i.[34] The DFT derived values for $G(x_i)$ were then fitted to the so-called universal binding energy relation,[35]

$$G(x) = G_c\left[1 - \left(1 + \frac{x}{l}\right)\exp\left(-\frac{x}{l}\right)\right]. \quad (2)$$

Utilizing the definition of the stress $\sigma(x)=dG(x)/dx$, the parameter l is the critical length, for which the stress reaches its maximum, the critical stress σ_c,

$$\sigma_c := \max\ \sigma(x) = \sigma(x=l) = \frac{G_c}{el}. \quad (3)$$

In general, the parameters G_c and l depend on the material and the orientation (hkl) of the actual cleavage plane. The critical stress σ_c represents the maximum tensile stress perpendicular to the given cleavage plane, which can be withstood without spontaneous cleavage. Because no relaxations are allowed, the procedure corresponds to uniaxial strain geometry of tensile loading. It should be noted that G_c and σ are implicitly divided by the area of the cleavage planes, as customarily done in the literature.

The calculated brittle cleavage properties of bulk VN and TiN for the three main low-index cleavage planes were included in the calculation. The results are displayed in Table V. It is very remarkable that critical stresses and cleavage energies vary strongly with direction, and for the (100) cleavage, the values are by far the smallest ones. The order of cleavage energies is according to the number of broken nearest-neighbor p-d bonds of the rocksalt lattice. One, two, and three p-d bonds for the (100), (110), and (111) orientations, respectively, are broken. This is directly related to the very short critical length l, which is typical for cubic refractory compounds [such as the studied nitrides, VC, and TiC (Refs. 34 and 36)]. Clearly, the remarkably small value of l indicates the brittleness of these materials, which presumably breaks preferable between (100) planes (at least under mode I loading). Planes of (111) orientation are by far the hardest to cleave. Such a cleavage would separate pure monatomic planes containing either the metal or nitrogen only.

The curious bonding properties of VN and TiN (and related compounds) are revealed by an approximate expression for the critical stress σ_c' in terms of the cleavage energy G_c and the uniaxial stress C,

TABLE V. Calculated brittle cleavage properties of bulk VN and TiN: orientation (*hkl*), cleavage energy G_c (in J/m^2), critical length l (in Å), uniaxial modulus C (Ref. 24), critical stress σ_c, and critical stress σ_c' (all in GPa) derived from a simplified model (Ref. 34).

	[*hkl*]	G_c	l	C	σ_c	σ_c'
VN	(100)	2.6	0.37	636	25	31
	(110)	5.0	0.52	525	36	39
	(111)	7.4	0.54	488	51	46
TiN	(100)	3.0	0.39	604	28	32
	(110)	6.0	0.53	532	42	43
	(111)	9.5	0.57	508	61	53

$$\sigma_c' \approx 0.24\sqrt{CG_c}. \tag{4}$$

[Naturally, all quantities depend on the orientation (*hkl*), and σ_c' and G_c are implicitly divided by the area of the cleavage plane.] This model was derived from DFT calculations, utilizing the concept of localized elastic energy. For more details, we refer the reader to Ref. 34. Table V shows that the estimation of Eq. (4) describes the direction-dependent trend of critical stresses reasonably well. Although the modulus C is the largest for the (100) orientation, the corresponding critical stress σ_c' is the smallest, because of G_c, which is the smallest for the (100) case. This indicates stiff but brittle bonds. The useful results of Eq. (4) clearly demonstrate that there is no general, universal relation for cleavage (fracture) properties solely expressed in terms of elastic properties: on the right side of the equation, we find the product of an elastic modulus and the cleavage energy.

To our knowledge, no reliable experimental fracture data for bulk refractory nitrides such as VN and TiN are available. Results for thin film layers, however, are published. There is an experimental report about fabricating bulk TiN,[37] but the mechanical properties of the samples depend strongly on the sintering conditions. One should be cautious to compare the critical stresses of Table V directly to hardness measurements (e.g., Refs. 1 and 38) because our calculations refer to single crystals of ideal stoichiometry as cleaved by an uniaxial loading of mode I.

IV. VN/TiN MULTILAYER

A. Strain and interface energy

Because of the significantly different lattice parameters of VN and TiN (the value for TiN is about 3% larger), there are sizeable strain effects when a coherent multilayer system with a common lateral lattice parameter is formed. According to elasticity theory, the formation of a coherent interface between the two mismatched parts is accompanied by uniaxial strains of both parts. In order to characterize the strained state enforced by various substrates, we calculated the strain energy $\Delta E_{st}(a_{lat})$ as a function of the lateral lattice parameter a_{lat} for the (100) planes,

$$\Delta E_{st}(a_{lat}) = E(a_{lat}) - E_0, \tag{5}$$

in which E_0 is the energy of the unstrained material. Such calculations were performed for the pure bulk phases of VN and TiN, as well as for the multilayer system VN/TiN by fixing the lateral lattice parameter a_{lat} and letting the unit cell relax in the [001] or z direction. By that, we can model epitaxy of thick blocks of materials on substrates with (100) fcc surfaces without considering the chemical interaction between substrate and grown material. According to Fig. 2, the strain energy per layer has a minimum at $x \approx 4.18$ Å somewhat smaller than the average of the bulk lattice parameter of 4.20 Å due to the additional compressive strain of the free surfaces of geometry model (a). Considering the bulk geometry model (b), one finds 4.195 Å for alternating blocks of six layers which increases to 4.20 Å for 15 layer blocks, approaching a value of 4.207 Å for very thick layer blocks as derived from the bulk data shown in Fig. 2. If growth on MgO(100) (a_{lat}=4.22 Å) is assumed, then the whole multilayer experiences a tensile strain which costs about 0.04 eV per layer. The strain energy induced for the lattice parameter of Al is considerably larger, indicating that growth of perfect stoichiometric VN(100)/TiN(100) multilayers on Al(100) is unfavorable, and presumably only thin layers might grow in a well-ordered way. The strain energy may be dissipated, for instance, by stretching softer Al to match the dimensions of VN or by increasing the concentration of nitrogen vacancies in VN, because it is well known that transition metal nitrides may contain up to 20% vacancies in the

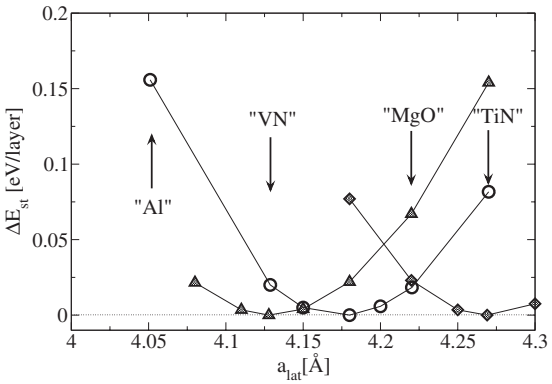

FIG. 2. Strain energy $\Delta E_{st}(a_{lat})$ per (100) layer vs lateral lattice parameter a_{lat} for (100) planes of materials with fcc structure: ○, VN/TiN slab consisting of six layers for each nitride according to model a); ◇, bulk TiN; and △, bulk VN. Arrows mark the lateral parameters corresponding to the bulk lattice parameters of some selected materials (as denoted within the quotation marks).

nitrogen sublattice.[39] For TiN_x, significant changes of the lattice parameter were observed.[40] For VN_x films, the rock-salt structure is stable for a broad range of the nitrogen concentration and it is found that the average lattice parameters derived from x-ray diffraction data are decreasing with decreasing nitrogen content.[41]

Considering the strain energy for the bulk phases, one realizes that at the lateral parameter of MgO(100), the strain energy for pure VN is more than twice as large as for pure TiN. One may estimate how many layers of the strained but otherwise perfect material might grow on a substrate by considering the total strain energy for a block of n bulklike layers, which is $n\Delta E_{st}(a_{lat})$. (It should be noted that ΔE_{st} is the strain energy per layer according to Fig. 2.) If the total strain energy equals the chemical bonding energy at the interface or surface, then the strain energy might dissipate in other ways, e.g., by misfit dislocations. The mentioned chemical energy can be derived from the cleavage energy at the interface, which in our case is $G_c=3.2$ eV for $a_{lat}=4.22$ Å corresponding to MgO(100). Because for VN at this lateral parameter, the strain energy per layer is $\Delta E_{st}^{\mathrm{VN}}=0.067$ eV, whereas for TiN, we derive $\Delta E_{st}^{\mathrm{TiN}}=0.023$ eV, the critical layer numbers of ≈ 50 layers for VN and ≈ 140 for TiN can be calculated. As reported by Helmersson *et al.*,[1] for layer thicknesses ranging from 0.75 to 16 nm (i.e., approximately from 4 to 76 atomic layers), the VN/TiN single-crystal multilayers grew coherent with no evidence of misfit dislocation arrays, in accordance with our estimate. Of course, the above estimate is rather an upper boundary of the critical thickness, since the misfit energy of the dislocation is usually lower than the cleavage energy.[10]

Based on the calculations above, the Poisson ratio for (001) oriented samples can be predicted. The TiN layer is compressed by an in-plane strain of $\epsilon_{\parallel}=-0.0328$ in order to match to the smaller spacing of MgO. This in-plane strain results in a strain of $\epsilon_{\perp}=0.0201$ perpendicular to the interface as a result of a calculation for fixed $a_{lat}=4.22$ Å and relaxed [001] or z axis. The Poisson ratio is then derived from the relation

$$\nu = \frac{\epsilon_{\perp}/\epsilon_{\parallel}}{\epsilon_{\perp}/\epsilon_{\parallel} - 2}. \tag{6}$$

For TiN, the result of $\nu=0.235$ agrees very well with the averaged value in Table IV as well as with a current experimental result $\nu=0.23\pm0.03$ obtained from a technique combining impact excitation and depth-sensing indentation.[31] Performing analogous calculation for VN, a value of $\nu=0.279$ is obtained. This value is exactly the average Voigt's and Reuss's estimates listed in Table IV. There exists, however, no experimental reference with which we could compare our results.

The interface energy γ per interface area A is defined as the difference between the total energy $E_{\mathrm{VN/TiN}}$ of the combined VN/TiN multilayer system and the total energies E_{VN}^{layer} and E_{TiN}^{layer} of the corresponding n bulk like layers of VN and TiN,

$$\gamma = (E_{\mathrm{VN/TiN}} - nE_{\mathrm{VN}}^{layer} - nE_{\mathrm{TiN}}^{layer})/A. \tag{7}$$

For the actual calculation of γ, it was assumed that VN/TiN multilayers were grown on MgO(100) substrate. Consequently, an overall lateral lattice parameter $a_{lat}^{\mathrm{MgO}}=4.22$ Å was fixed, corresponding to the calculated bulk lattice parameter of MgO. With respect to the equilibrium lattice parameters of bulk VN and TiN (see Tables I and II), VN(100) layers have to be stretched laterally, whereas TiN(100) layers contract in order to match the MgO(100) epitaxial conditions. Finally, for the calculation of the interface energy, the VN/TiN multilayer system was allowed to relax along the z axis in order to minimize the total energy. The bulk layer energies may be derived from bulk calculations with suitable supercells which are constructed by stacking of (100) planes. For the interface energy, we finally derived a value of $\gamma=-0.054$ J/m^2. Its very small absolute value indicates that the creation of the described VN/TiN interface is very favorable, because VN and TiN (100) layers are rather similar concerning their bonding properties. The negative sign arises because the bulk layer energies were derived for strained VN and TiN layers, as described above. Taking bulk layer energies for the respective unstrained cases of VN and TiN increases the interface energy up to $\gamma=0.35$ J/m^2.

A DFT study for Fe[011](100)/VN[001](100) interfaces reports that a single VN layer has an interface energy of 0.245 J/m^2, whereas for thicker VN slabs, even negative values of the interface energy were derived.[42] When comparing these results to our study, one should note that our calculations were made for rather thick slabs consisting of six layers for each nitride block. All the results indicate that the actual value of the interface energy strongly depends on the straining conditions which the (multi)layers have to obey.

Because of the simple (100) fcc geometry, most of the structural relaxation affects the interlayer distances. The rumpling within the VN and TiN planes at the interface is rather small: the Ti-N distance is 2.19 Å and the N-V distance is 2.09 Å. According to Fig. 3, in the VN block the interlayer distances show strong periodic relaxations around the bulk value in the range of 0.025–0.3 Å which is about 12%–14% of the bulk interlayer spacing. For the TiN block, the relaxation are much smaller. The periodic behavior of VN is not an artifact due to the size of the VN block. Actually, we obtained the same periodic relaxation also for a block containing 15 layers of VN. This relaxation deforms the VN layers into a structure with tetragonal-like stacking, in which narrowly and widely spaced pairs of planes are created. Notice that this relaxation follows as a reaction to epitaxial strain acting on VN. One may consider it as an indication of an *instability against tetragonal distortion* in stoichiometric VN. Notably, for samples of nearly stoichiometric composition ($\mathrm{N/V}>0.99$), the transformation of the NaCl structure into a tetragonal, noncentrosymmetric low temperature modification was already observed,[43] and confirmed by our DFT calculations to be more stable by 0.036 eV/f.u. Hence, a NaCl phase of VN in its stoichiometric form may be only metastable. The structure could be stabilized, for instance, by creating nitrogen vacancies, which agrees well with the experimental difficulty to synthesize NaCl-type VN samples close to stoichiometry.

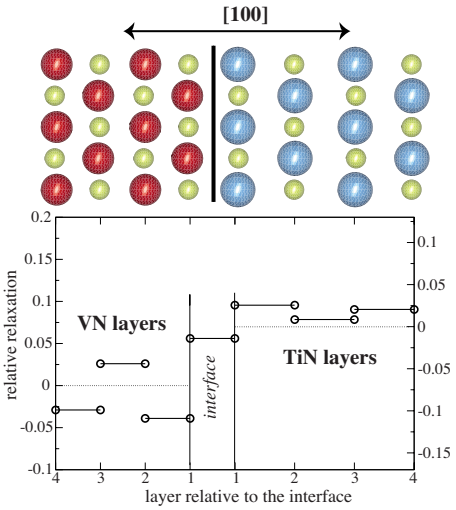

FIG. 3. (Color online) Relaxation of averaged, $(z^{(\mathrm{Ti,V})}+z^{\mathrm{N}})/2$, interlayer distances (in Å) of VN(100)/TiN(100) multilayers for the overall lateral lattice parameter $a_{lat}^{\mathrm{MgO}}=4.22$ Å. Dashed lines indicate the spacings for the equilibrium bulk phases. A model of the interface is shown on top: small spheres denote N and large spheres V and Ti, respectively.

B. Brittle cleavage properties

The brittle cleavage properties at the interface for VN/TiN multilayers at the lateral lattice parameter of $a_{lat}=4.22$ Å of MgO(100) are studied in order to investigate the difference to the cleavage properties of the single phases of VN and TiN. The calculations were done in the same way as described in Sec. III B. Before cleaving, the lateral lattice parameter for the VN/TiN multilayer was fixed to $a_{lat}=4.22$ Å according to MgO(100) but the structure was relaxed in the [001] direction.

According to Table VI, the cleavage energy of the VN/TiN interface is approximately the average of the cleavage energies of VN and TiN in the interior regions. Comparing the cleavage properties of VN and TiN in the interior of the slab to the bulk phases with (100) orientation in Table V, one realizes that TiN is weakened with respect to VN. By compressing TiN to the lateral parameter of MgO(100), its cleavage energy decreases, whereas for stretched VN, the effect is opposite. As described in the previous section, this is due to the different perpendicular strains occurring in these two blocks which is also realized from Fig. 3: the first interlayer distance for the VN block is strongly contracted by 0.04 Å, whereas for TiN, it is enlarged by only 0.02 Å.

TABLE VI. Calculated brittle cleavage properties for the [001] direction of the VN(100)/TiN(100) multilayer system at the lateral lattice parameter of $a_{lat}=4.20$ Å of MgO(100): cleavage energy G_c, critical length l, and critical stress σ_c. For more details, see Sec. III B.

	G_c (J/m^2)	l (Å)	σ_c (GPa)
VN interior	3.3	0.37	33
VN/TiN interface	3.0	0.39	27
TiN interior	2.7	0.40	25
TiN/MgO interface	1.8	0.39	16

TABLE VII. Calculated brittle cleavage properties at the interface for the [001] direction of the VN(100)/TiN(100) multilayer system at varying lateral lattice parameters a_{lat}: cleavage energy G_c, critical length l, and critical stress σ_c. For more details, see Sec. III B.

a_{lat} (Å)	G_c (J/m^2)	l (Å)	σ_c (GPa)
4.128 (VN)	3.13	0.407	27.7
4.18	3.08	0.411	27.0
4.22	2.91	0.387	27.1
4.27 (TiN)	2.66	0.370	25.9

The weakest part of the system is the TiN/MgO interface with its cleavage of 1.8 J/m^2, which is comparable to the cleavage energy (which is twice the surface energy) of pure MgO(100). This result is in quantitative agreement with other DFT based studies of nitride and/or metal adhesion. For the Al(100)/VN(100) interface, an adhesion energy of 1.68 J/m^2 was calculated, for which Al was strained to match the dimensions of bulk VN.[8]

In the case of the VN/TiN interfacial cleavage, we also explored an influence of the coherency strains on the cleavage strength of the interface. For that, we calculated cleavage profiles at various values of a_{lat} (see previous section for details). Observing the results in Table VII, one realizes a pronounced change of G_c when going from the lattice parameter of VN to that of TiN. Interestingly, the critical cleavage stress is much less changed. The key factor is l, as its shrinking compensates the changes of G_c and stabilizes the critical stress at values around 27 GPa for a_{lat} varying from in the sizeable range of 4.13–4.22 Å. This behavior indicates that the cleavage strength of the VN/TiN interface is not supposed to change much with respect to various substrates if their lateral parameters are in the described range.

V. SUMMARY

We performed a DFT study of the properties of VN(100)/TiN(100) multilayered superlattice system. For the bulk single-crystalline phases of VN and TiN, strong anisotropies of the brittle cleavage properties as well as the elastic properties were found. The anisotropy is due to the strong bonds between N and the transition metals in the [100] direction of the rocksalt structure. The lowest cleavage energy is derived for (100) planes. Both materials exhibit remarkably high critical stresses for the (111) cleavage faces, namely, 51 and 61 GPa for VN and TiN, respectively. In contrast to the rather weak cleavage properties of the (100) planes, the uniaxial elastic modulus is largest for the [001] direction for both VN and TiN.

Our idealized model revealed that the strengthening observed in multilayers is not directly connected to a change of

the cleavage properties. The cleavage energy of the interface is an average between the energies of both materials. According to our calculation, the role of different substrates can be excluded as well, because upon a rather large change of the lateral spacing of the multilayer within 4.13–4.27 Å, no significant effect on the cleavage properties of the multilayer interface can be derived. Assuming multilayer growth on an Mg(100) substrate [i.e., fixing the lateral parameter to the calculated value of 4.20 Å of MgO(100)], the cleavage energy of VN is enlarged by 10%, whereas it decreases for TiN. This is a consequence of strains in the coherently matched VN/TiN multilayer slab, because after stretching VN to match the MgO lattice parameter, its spacing in the direction normal to the interface shrinks, thus improving its cohesive properties in the [001] direction. For TiN, the effect is opposite, because it has to compressed to match the epitaxial conditions of the MgO substrate.

According to our results calculated for an ideal interface of a perfectly matched VN(100)/TiN(100) multilayer, no major increase of the cleavage properties may be expected from such coatings with perfect interface conditions. A major increase in the cleavage stress of a realistic material may be expected if extensive dislocations and fracture in the [001] directions are hindered because the critical stresses for [011] and, in particular, for [111] directions are significantly larger than for the [001] cases for both nitrides.

For the multilayer system VN(100)/TiN(100), the calculation of the strain energy induced by different substrates reveals that the MgO(100) substrate—as commonly used in epitaxial experiments—provides a low coherency stress partially due to the softer bonding in VN: At a lateral lattice parameter corresponding to bulk VN, the strain energy is considerably smaller than at that of bulk TiN. Furthermore, the relaxation of atoms following an epitaxial strain of VN layers deforms VN into the structure with tetragonal-like stacking; narrowly and widely spaced pairs of planes are created. This fact is an indication that stoichiometric VN is *metastable* against tetragonal distortion.

By compressing the TiN(100) layer to be lattice matched with VN(100), we evaluated the Poisson ratio. The value of $\nu=0.235$ agrees well with a current experimental result $\nu=0.23\pm0.03$. A similar calculation for VN yields $\nu=0.279$, which seems to be useful, because no experimental value is available. Knowledge of Poisson's ratio is extremely important for the characterization of coatings, as it is needed to determine the mechanical properties of coatings in techniques such as depth-sensing indentation and surface acoustic wave spectroscopy.

For the TiN(100)/MgO(100) interface, a cleavage energy of 1.8 J/m^2 was calculated. Comparing to the other theoretical results for nitride interfaces with Al and Fe, one can conclude that MgO substrates should be better suited. The TiN(100)/MgO(100) multilayer system has a larger cleavage energy and, according to our strain energy calculation, by epitaxial growth of VN/TiN multilayers a relatively low coherency stress is induced. Finally, the interface energy for epitaxial growth on MgO(100) is rather favorable, namely, -0.054 J/m^2. The negative sign arises because the bulk layer energies were derived for strained VN and TiN layers.

ACKNOWLEDGMENT

This work was supported by the Austrian NANO Initiative via a grant from the Austrian Science Fund FWF within the project "N404 Modeling and experimental studies of VN/TiN interfaces and surfaces."

APPENDIX

For a cubic structure, the uniaxial modulus C is defined in terms of the elastic constants c_{11}, c_{12}, and c_{44} by

$$C = c_{11} - 2(c_{11} - c_{12} - 2c_{44})(h^2k^2 + h^2l^2 + k^2l^2). \quad \text{(A1)}$$

The corresponding compliances s_{11}, s_{12}, and s_{44} are obtained given by[25]

$$s_{11} = \frac{c_{11} + c_{12}}{(c_{11} - c_{12})(c_{11} + 2c_{12})}, \quad \text{(A2)}$$

$$s_{12} = \frac{-c_{12}}{(c_{11} - c_{12})(c_{11} + 2c_{12})}, \quad \text{(A3)}$$

$$s_{44} = \frac{1}{c_{44}}. \quad \text{(A4)}$$

The general methodology of averaging the elastic constants is outlined, e.g., in Ref. 44. We used the procedures according to Voigt and Reuss which provide upper and lower bounds for the averaged bulk and shear modulus. For a cubic crystal, Voigt's average results in relations for the Lamé constant λ and the shear modulus μ,

$$\mu = c_{44} - \frac{1}{5}H, \quad \text{(A5)}$$

$$\lambda = c_{12} - \frac{1}{5}H, \quad \text{(A6)}$$

in which H is the anisotropy factor given as $H=2c_{44}+c_{12}-c_{11}$. From Reuss's average for elastic compliances, the relations

$$\frac{1}{E} = s_{11} - \frac{2}{5}J, \quad \text{(A7)}$$

$$\frac{1}{\mu} = s_{44} + \frac{4}{5}J \quad \text{(A8)}$$

are derived in which E is the elastic modulus and $J=s_{11}-s_{12}-\frac{1}{2}s_{44}$. Poisson's ratio of an isotropic material is then defined by

$$\nu = \frac{E - 2\mu}{2\mu}. \quad \text{(A9)}$$

*pl@cms.tuwien.ac.at

[1] U. Helmersson, S. Todorova, S. A. Barnett, J. E. Sundgren, L. C. Markert, and J. E. Greene, J. Appl. Phys. **62**, 481 (1987).
[2] P. B. Mirkarimi, L. Hultman, and S. A. Barnett, Appl. Phys. Lett. **57**, 1654 (1990).
[3] M. Shinn, L. Hultman, and S. A. Barnett, J. Mater. Res. **7**, 901 (1992).
[4] X. Chu and S. A. Barnett, J. Appl. Phys. **77**, 4403 (1995).
[5] J. W. Cahn, Acta Metall. **11**, 1275 (1963).
[6] M. Kato, T. Mori, and L. H. Schwartz, Acta Metall. **28**, 285 (1980).
[7] J. Hartford, Phys. Rev. B **61**, 2221 (2000).
[8] D. J. Siegel, L. G. Hector, and J. B. Adams, Acta Mater. **50**, 619 (2001).
[9] D. J. Siegel, L. G. Hector, and J. B. Adams, Phys. Rev. B **67**, 092105 (2003).
[10] N. I. Medvedeva, Y. N. Gornostyrev, O. Y. Kontsevoi, and A. J. Freeman, Acta Mater. **52**, 675 (2004).
[11] A. A. Griffith, Philos. Trans. R. Soc. London, Ser. A **221**, 163 (1921).
[12] J. O. Kim, J. D. Achenbach, P. B. Mirkarimi, M. Shinn, and S. A. Barnett, J. Appl. Phys. **72**, 1805 (1992).
[13] D. Gall, I. Petrov, P. Desjarins, and J. E. Greene, J. Appl. Phys. **86**, 5524 (1999).
[14] P. E. Blöchl, Phys. Rev. B **50**, 17953 (1994).
[15] G. Kresse and D. Joubert, Phys. Rev. B **59**, 1758 (1999).
[16] J. P. Perdew and Y. Wang, Phys. Rev. B **45**, 13244 (1992).
[17] C. Stampfl, W. Mannstadt, R. Asahi, and A. J. Freeman, Phys. Rev. B **63**, 155106 (2001).
[18] W. Wolf, R. Podloucky, T. Antretter, and F. D. Fischer, Philos. Mag. B **79**, 839 (1999).
[19] W. B. Pearson, *A Handbook of Lattice Spacings and Structures of Metals and Alloys* (Pergamon, Oxford, 1967), Vol. 2.
[20] R. Ahuja, O. Eriksson, J. M. Wills, and B. Johansson, Phys. Rev. B **53**, 3072 (1996).
[21] M. Zhang and J. He, Surf. Coat. Technol. **142**, 125 (2001).
[22] H. Krakauer, M. Posternak, and A. J. Freeman, Phys. Rev. B **19**, 1706 (1979).
[23] J. P. Perdew, J. A. Chevary, S. H. Vosko, K. A. Jackson, M. R. Pederson, D. J. Singh, and C. Fiolhais, Phys. Rev. B **46**, 6671 (1992).
[24] For example, for a cubic structure the modulus for any direction is given by $C[hkl]=c_{11}-2(c_{11}-c_{12}-2c_{44})(h^2k^2+h^2l^2+k^2l^2)$.
[25] J. F. Nye, *Physical Properties of Crystals* (Oxford University Press, Oxford, 1993).
[26] D. Legut, M. Friák, and M. Šob, Phys. Rev. Lett. **99**, 016402 (2007).
[27] E. Török, A. J. Perry, L. Chollet, and W. D. Sproul, Thin Solid Films **153**, 37 (1987).
[28] M. Wittling, A. Bendavid, P. J. Martin, and M. V. Swain, Thin Solid Films **270**, 283 (1995).
[29] R. Gunda, S. K. Biswas, S. Bhowmick, and V. Jayram, J. Am. Ceram. Soc. **88**, 1831 (2005).
[30] J. C. Knight and T. F. Page, Thin Solid Films **193**, 431 (1990).
[31] A. S. Maxwell, S. Owen-Jones, and N. M. Jennett, Rev. Sci. Instrum. **75**, 970 (2004).
[32] G. M. Pharr, W. C. Oliver, and F. R. Brotzen, J. Mater. Res. **7**, 613 (1992).
[33] D. Schneider and T. Schwarz, Surf. Coat. Technol. **91**, 136 (1997).
[34] P. Lazar, R. Podloucky, and W. Wolf, Appl. Phys. Lett. **87**, 261910 (2005).
[35] J. H. Rose, J. R. Smith, and J. Ferrante, Phys. Rev. B **28**, 1835 (1983).
[36] J. Gilman and B. Roberts, J. Appl. Phys. **32**, 1405 (1961).
[37] H. Kuhawara, N. Mazaki, M. Takahashi, T. Watanabe, X. Yang, and T. Aizawa, Mater. Sci. Eng., A **319**, 687 (2001).
[38] B. A. Latella, B. K. Gan, K. E. Davies, D. R. McKenzie, and D. G. McCulloch, Surf. Coat. Technol. **200**, 3605 (2006).
[39] L. E. Toth, *Transition Metal Carbides and Nitrides* (Academic, San Diego, CA, 1971).
[40] J. E. Sundgren, Thin Solid Films **128**, 21 (1985).
[41] R. Sanjinés, C. Wiemer, P. Hones, and F. Lévy, J. Appl. Phys. **83**, 1396 (1988).
[42] J. Hartford, B. von Sydow, G. Wahnström, and B. I. Lundqvist, Phys. Rev. B **58**, 2487 (1998).
[43] F. Kubel, W. Lengauer, K. Yvon, K. Knorr, and A. Junod, Phys. Rev. B **38**, 12908 (1988).
[44] J. Hirth and J. Lothe, *Theory of Dislocations* (McGraw-Hill, New York, 1968).